

# Test of isospin symmetry via low energy ${}^1\text{H}(\pi^-, \pi^0)n$ charge exchange

Y. Jia,<sup>1</sup> T. P. Gorringer,<sup>1</sup> M. D. Hasinoff,<sup>2</sup> M. A. Kovash,<sup>1</sup> M. Ojha,<sup>1</sup> M.M. Pavan,<sup>3</sup> S. Tripathi,<sup>1</sup>  
P. A. Żołnierczuk,<sup>1</sup>

<sup>1</sup> University of Kentucky, Lexington, KY 40506 <sup>2</sup> University of British Columbia, Vancouver, B.C., Canada V6T 1Z1

<sup>3</sup> TRIUMF, 4004 Wesbrook Mall, Vancouver, B.C., Canada V6T 2A3

(November 1, 2018)

We report measurements of the  $\pi^-p \rightarrow \pi^0n$  differential cross sections at six momenta (104-143 MeV/c) and four angles (0-40 deg) by detection of  $\gamma$ -ray pairs from  $\pi^0 \rightarrow \gamma\gamma$  decays using the TRIUMF RMC spectrometer. This region exhibits a vanishing zero-degree cross section from destructive interference between s- and p-waves, thus yielding special sensitivity to pion-nucleon dynamics and isospin symmetry breaking. Our data and previous data do not agree, with important implications for earlier claims of large isospin violating effects in low energy pion-nucleon interactions.

13.75.Gx,25.80.Gn

Studies of pion-nucleon dynamics have long played a central role in nuclear physics. For example, the  $\pi\text{N}$  system enables important tests of basic symmetries – notably isospin symmetry and chiral symmetry – that are fundamental to the low energy realization of the strong force. Interestingly, the possibility of gross violations of isospin symmetry in  $\pi\text{N}$  processes involving neutral pions was first suggested by Weinberg [1].

Of the eight possible  $\pi\text{N} \rightarrow \pi\text{N}$  channels there are three experimentally accessible channels:  $\pi^+p$  elastic scattering,  $\pi^-p$  elastic scattering and  $\pi^-p \rightarrow \pi^0n$  charge exchange (CEX). Assuming isospin symmetry, the three hadronic amplitudes for the three channels are determined by two isospin amplitudes, thus implying a triangle relationship among the amplitudes  $f_{\text{CEX}} = (f_- - f_+)/\sqrt{2}$ . Consequently, an important test of isospin symmetry is possible by comparing the extracted amplitude,  $f_{\text{CEX}}$ , from CEX data, with the predicted amplitude,  $f'_{\text{CEX}} \equiv (f_- - f_+)/\sqrt{2}$ , from elastic data.

Special sensitivity to isospin violation in  $\pi\text{N}$  interactions is afforded by pion CEX at forward angles and 100-150 MeV/c. At these kinematics the dominating s- and p-waves interfere destructively and yield a striking dip in the cross section [2]. This cancellation of the isospin conserving amplitude thus amplifies the sensitivity to possible isospin non-conserving amplitudes, thereby allowing a delicate test of symmetry breaking.

A comparison between the scattering amplitudes predicted from elastic data ( $f'_{\text{CEX}}$ ) and those extracted from CEX data ( $f_{\text{CEX}}$ ) was made by Gibbs *et al.* [4,5] and Matsinos *et al.* [6,7]. While different in details, both studies found evidence of an unexpectedly large isospin violation after accounting for the effects of  $\pi^\pm p$  Coulomb

interactions and hadronic mass differences (we note this conclusion was questioned in Refs. [8,9]). In particular, both Gibbs *et al.* and Matsinos *et al.* reported a  $-0.012 \pm 0.003$  fm discrepancy between the forward scattering amplitudes that are extracted from the CEX data and those predicted from the elastic data.

Subsequently, Piekarewicz [10] claimed that a symmetry breaking originating in the u,d-quark mass difference may explain these results. In Piekarewicz's calculation the u,d-quark mass difference induces inequalities among the  $\pi^0p$ ,  $\pi^0n$  and  $\pi^\pm\text{N}$  couplings that are realized as a  $-0.015$  fm correction to the triangle relationship. However Fettes and Meissner [11], using chiral perturbation theory, have concluded quark mass differences yield much smaller isospin breaking effects in the  $\pi\text{N}$  interaction.

While the elastic dataset is extensive and precise, the CEX dataset is more limited and less accurate [12]. Most notably, the region of momenta 100-150 MeV/c and forward angles is dominated by a single experiment due to Fitzgerald *et al.* [2] (an additional experiment by Isenhower *et al.* [3] has reported preliminary data at 112 MeV/c). The Fitzgerald experiment used the LAMPF  $\pi^0$  spectrometer and measured cross sections at momenta 100.6-147.1 MeV/c and angles  $\theta < 25$  degrees. Unfortunately, both the absolute normalization, obtained from  ${}^{12}\text{C}(\pi, \pi\text{N}){}^{11}\text{C}$  activation measurements, and the background subtraction, determined from  ${}^{12}\text{C}(\pi^-, \pi^0)$  background measurements, have been questioned [3,13].

Given the importance of the cross section minimum as an isospin symmetry test we undertook a new measurement of CEX differential cross sections at momenta 104-143 MeV/c and angles 0-40 degrees. Our experiment was conducted using the RMC detector on the M9A beamline at the TRIUMF cyclotron. The RMC detector is a large acceptance pair spectrometer that was developed for radiative muon capture studies [14].

The M9A beamline provided a pion flux of  $1.9-2.5 \times 10^6 s^{-1}$  with  $e/\mu$  contamination of 28-58% for momenta 104-143 MeV/c. The spot size was about  $3 \times 3$  cm<sup>2</sup> (FWHM) and the momentum bite was about 6 MeV/c (FWHM). Note that the primary proton beam comprised pulses of duration 2-4 ns and separation 43 ns, and therefore the arrival of  $\pi$ 's,  $\mu$ 's and  $e$ 's were time-separated.

Beam particles were registered in two plastic scintillators before traversing the target. The upstream counter (B1) was 6.0 cm diameter and 0.3 cm thick and the downstream counter (B2) was 6.0 cm diameter and 0.15 cm

thick. The targets were disks of polyethylene ( $\text{CH}_2$ ) and carbon (C) of diameter 7.0 cm and thickness 1.2 cm.

Neutral pions were identified by detecting the two photons from  $\pi^0 \rightarrow \gamma\gamma$  decay using the RMC spectrometer. The  $\text{CH}_2/\text{C}$  targets were located about 40 cm upstream of the geometrical center of the RMC spectrometer, thus permitting the detection of forward-going photon pairs from forward angle CEX. The photons were detected by  $\gamma \rightarrow e^+e^-$  conversion in a cylindrical lead converter of thickness 1.7 mm, radius 24.7 cm and length 60.0 cm. The resulting  $e^+e^-$  pairs were tracked in a low mass cylindrical multi-wire chamber and a large volume cylindrical drift chamber. A four-fold segmented, doubled-layered ring of veto scintillators (the A/A' ring), located within the Pb radius, was used to reject backgrounds from charged particles. A sixteen-fold segmented, single-layered ring of trigger scintillators (the D ring), located outside the drift chamber radius, was used to identify  $e^\pm$ 's from  $\gamma$ -ray conversions. A large solenoid provided a 2.206 kG axial magnetic field thus enabling the momentum analysis of charged particles.

The  $\pi^0$  trigger required coincident hits in the two beam counters, zero hits in the A/A'-ring, and  $\geq 3$  hits in the D-ring. The  $\pi^0$  trigger also imposed a requirement of  $\geq 3$  cell hits in drift chamber layer 2 and  $\geq 6$  cell clusters in drift chamber layers 3+4. In addition, a beam trigger was derived by prescanning the B1-B2 coincidences and used to continuously monitor the beam properties. On fulfilling either trigger the acquisition read out the chamber hits and times and the scintillator ADCs and TDCs.

A stopping  $\pi^-$  beam and liquid  $\text{H}_2$  target were used for the spectrometer calibration via at-rest  $\pi^-p \rightarrow \pi^0n$  using the well-known Panofsky ratio [15]. The stopping beam had a momentum of 81 MeV/c and the hydrogen target was a cylindrical cell of 16 cm diameter and 15 cm length with 0.25 mm thick Au walls.

Our data was collected at six momenta with central values 103.8, 112.9, 118.3, 123.8, 134.4 and 142.8 MeV/c. At each momenta setting we made measurements with the  $\text{CH}_2$ , C transmission targets and an empty target setup, and collected all scattering angles simultaneously.

The analysis was organized as follows. First, we applied beam, tracking, photon and  $\pi^0$  cuts to identify the photon pairs from  $\pi^0 \rightarrow \gamma\gamma$  decays. Next, for each  $\pi^-$  momentum setting and  $\pi^0$  angle range, the number of  ${}^1\text{H}(\pi^-, \pi^0)$  events was extracted via a fitting procedure using the  $\text{CH}_2$ , C, and empty target momentum spectra. Finally, from a simulation of the in-flight CEX detection efficiency, and the measurement of the at-rest CEX detection efficiency, we normalized the  ${}^1\text{H}(\pi^-, \pi^0)$  events and determined the cross sections.

The event reconstruction first assembled chamber hits into candidate tracks, then paired  $e^+e^-$  tracks into candidate photons, and finally paired photons into candidate  $\pi^0 \rightarrow \gamma\gamma$  events. A beam cut imposed requirements on the minimum amplitudes of the pulse heights in the two

beam counters. A tracking cut imposed requirements on the minimum points and the maximum variances in the fits to the helical  $e^+$ ,  $e^-$  trajectories in the tracking chambers. A photon cut required that the  $e^+$  and  $e^-$  tracks converge at the Pb converter, and a  $\pi^0$  cut required that the photon-pair converge at the target.

The data at each momentum were divided into four angle bins with scattering angles 0-10, 10-20, 20-30 and 30-40 degrees, thus yielding twenty-four data points. Representative  $\pi^0$  momenta spectra for the  $\text{CH}_2$  and C targets are shown in Fig. 1. The  $\text{CH}_2$  spectra show a peak from the  ${}^1\text{H}(\pi^-, \pi^0)$  reaction and a continuum from the  ${}^{12}\text{C}(\pi^-, \pi^0)$  reaction. At forward angles the  ${}^1\text{H}$  peak and  ${}^{12}\text{C}$  background were kinematically separated while at larger angles the contributions were overlapping.

To obtain the number of  ${}^1\text{H}(\pi^-, \pi^0)$  events we performed fits of the measured  $\text{CH}_2$  spectra to the sum of a simulation of the  ${}^1\text{H}(\pi^-, \pi^0)$  lineshape and the measurement of the  $(\pi^-, \pi^0)$  background. Our benchmark fits (*e.g.* Fig. 1) involved one free parameter, the normalization constant for the  ${}^1\text{H}(\pi^-, \pi^0)$  lineshape. The background spectra for each angle-momentum bin was fixed by combining carbon and empty target spectra in accord with the target  $\pi^-$  exposures and areal densities.

Additional fits were made to quantify the systematic uncertainties associated with the  ${}^1\text{H}(\pi^-, \pi^0)$  lineshape,  $(\pi^-, \pi^0)$  background, *etc.* In one study we allowed the position of the  ${}^1\text{H}$  peak to be varied in the fit, and found a mean deviation of the  ${}^1\text{H}$  yields from the benchmark fits of  $0.51 \sigma$  (standard deviations). In a second study we allowed the amplitude of the background spectra to be varied in the fit, and found a mean deviation of the  ${}^1\text{H}$  yields from the benchmark fits of  $0.37 \sigma$ . In a third study we compared the results of fits either including or excluding a small correction for the 1.5-2.5 MeV/c differences in the  $\text{CH}_2$ -C target energy loss, and found a mean deviation of the  ${}^1\text{H}$  yields of  $0.22 \sigma$ . For the final uncertainties in the  ${}^1\text{H}$  yields we took the quadrature sum of the statistical errors from the benchmark fits with the maximum deviations from the supplementary fits.

The number of incident pions was determined by counting the B1-B2 coincidences and measuring the beam composition. The beam composition was determined using the beam trigger data and was based on the differences in the flight times and the pulse heights of the  $\pi^-$ 's,  $\mu^-$ 's and  $e^-$ 's. The largest uncertainty in the  $\pi^-$  flux determination was the beam composition measurement.

To derive the  ${}^1\text{H}(\pi^-, \pi^0)$  differential cross sections we required the spectrometer response function. The response function determines the probability of reconstructing a neutral pion of true momentum  $p_T$  and angle  $\theta_T$  with measured momentum  $p_M$  and angle  $\theta_M$ . It was computed via a simulation using the GEANT3 code [16]. The simulation incorporated the full geometry of the experimental setup and included the detailed interactions of the outgoing photons, conversion electrons, *etc.* The

same analysis package was used to process both simulated data and measured data.

The absolute normalization of the response function was obtained by comparing the measurement and simulation of at-rest CEX for the stopping  $\pi^-$  beam and the liquid  $H_2$  target. The energy-angle distributions of  $\gamma$ -pairs from at-rest CEX obtained from the measurement and the simulation were in excellent agreement. These comparisons were made for different trigger definitions, cut parameters, *etc.*, in order to fully test the detector simulation. However, the absolute efficiency for  $\pi^0$  detection was found to be smaller in the measurement than the simulation by a factor,  $F = 0.85 \pm 0.03$ . This difference is suspected to arise from contributions such as chamber noise and multiple pulsing that were absent in the simulation, and was observed in previous experiments with the RMC spectrometer. Importantly, at the level of the quoted uncertainty  $\pm 0.03$ , the factor  $F$  was independent of the trigger condition, cut parameters, photon energies and target position.

During production running the relative acceptance was monitored by measurements of at-rest CEX using a 2.5 cm thick  $CH_2$  target and an 81 MeV/c stopping  $\pi^-$  beam. The acceptance was found to be constant to about  $\pm 5\%$  over the duration of the experiment. Given the uncertainties in the determination of the absolute acceptance and the monitoring of the relative acceptance, an uncertainty of  $\pm 10\%$  was conservatively assigned to the overall normalization of the cross sections.

The measured cross sections are averages over the momentum dispersion of the beam and the momentum spread in the target. The beam momentum dispersion was obtained by analysis of the time-of-flight spectra of the incident beam particles. The target momentum spread was obtained by a GEANT3 simulation of the beam interactions in the target material. The typical beam dispersion was 2.8 MeV/c ( $\sigma$ ) and the typical target spread was 2.6 MeV/c ( $\sigma$ ). A correction (of 0.1-0.4  $\sigma$  in magnitude) was applied to convert the bin-averaged cross sections to bin-centered cross sections.

Our final results for the center-of-mass (CM) differential cross sections versus CM scattering angle and  $\pi^-$  laboratory momentum are plotted in Fig. 2. The error bars include the combined uncertainties in the  $\pi^-$  flux,  $^1H(\pi^-, \pi^0)$  yields, angular resolution and momentum interval, but omit the  $\pm 10\%$  normalization uncertainty.

Our data and earlier data near the minimum are in disagreement. Compared to Fitzgerald *et al.* [2] our cross sections are roughly factors of two smaller at momenta  $< 120$  MeV/c. This disagreement is beyond the quoted experimental uncertainties and – as discussed in Refs. [3,13] – may be related to the normalization procedure and the background subtraction in the Fitzgerald *et al.* experiment. At 113 MeV/c our results are also  $\sim 30\%$  smaller than the preliminary results of the Isenhower *et al.* experiment [3], although this discrepancy is statisti-

cally less significant.

Also plotted in Fig. 2 are the predicted cross sections from Gibbs *et al.* [4,5], Matsinos *et al.* [7] and the GWU group [12]. The Gibbs *et al.* analysis used a potential model where the parameters of the  $\pi N$  interaction were obtained by fitting the  $\pi^\pm p$  elastic dataset only. The predictions by Matsinos *et al.* and the GWU group were derived from partial wave analyses of the  $\pi^\pm p$  elastic dataset. We stress the GWU results in Fig. 2 are a ‘special solution’ based on  $T < 100$  MeV elastic data only – and differ slightly from their well-known SP06 solution [12]. All analyses include the isospin violation arising from Coulomb effects and hadronic mass splittings.

We first discuss the comparison among the Gibbs *et al.* and Matsinos *et al.* predictions and the CEX data – a comparison [4–7] that originally motivated claims of large isospin breaking effects in  $\pi N$  interactions. Fig. 2 shows our CEX data and these predictions are in quite good agreement, with Matsinos *et al.* being in agreement at all six momenta and Gibbs *et al.* being in agreement at the four lower momentum values and differing from our data by about 10-20% at the two higher momentum values. In contrast, the original comparisons of these predictions to the Fitzgerald *et al.* data showed large discrepancies. We therefore conclude our data contradict the original evidence for unexpected isospin violating effects.

However, the GWU results in Fig. 2 suggest some caution is necessary. Their results differ markedly from Gibbs *et al.* and Matsinos *et al.* in the dip region. Note these analyses do differ in details; for example in the omission and the normalizations of certain  $\pi^\pm p$  datasets. As mentioned by Matsinos *et al.* [7], such differences could result in small discrepancies in the s- and p-wave partial amplitudes that develop into large discrepancies in the CEX cross section. Thus final conclusions on isospin breaking will likely require a better understanding of such discrepancies.

Fig. 3 shows the extrapolated zero-degree cross sections derived from our data and Fitzgerald’s data. Although the extrapolated cross sections have larger uncertainties, they do allow for the direct comparison of the two experiments. Like Fitzgerald *et al.*, our extrapolations have assumed that the cross sections could be parameterized as second-order polynomials in  $\cos\theta_{CM}$ . Fig. 3 shows our data and Fitzgerald’s data are in clear disagreement for momenta below 120 MeV/c but closer agreement for momenta above 120 MeV/c. Moreover, while our data are reasonably consistent with Gibbs *et al.* and Matsinos *et al.* at all momenta, the Fitzgerald *et al.* data are obviously inconsistent with their predictions below 120 MeV/c. The GWU results are in greatest disagreement with our data at momenta  $< 120$  MeV/c and Fitzgerald’s data at momenta  $> 120$  MeV/c.

Last, we performed a fit of our zero-degree extrapolations to a second-order polynomial in the  $\pi^-$  momentum and found the minimum to be  $T_{min} = 41.9 \pm 0.9$  MeV.

Our result is in reasonable agreement with Gibbs *et al.* and Matsinos *et al.* which yield  $T_{min} \simeq 43$  MeV but in significant disagreement with the GWU result  $T_{min} \simeq 47$  MeV. The Fitzgerald *et al.* value  $T_{min} = 45.1 \pm 0.5$  MeV and our value  $T_{min} = 41.9 \pm 0.9$  MeV are in marginal disagreement.

In summary, we have measured the CEX differential cross section at six momenta (104-143 MeV/c) and four angles (0-40 deg.) using the TRIUMF RMC spectrometer. At momenta below 120 MeV/c our cross section measurements are considerably smaller than the published data of Fitzgerald *et al.* and somewhat smaller than the preliminary data of Isenhower *et al.* Interestingly, our results are consistent with the cross sections derived from the low energy  $\pi^\pm p$  elastic dataset by Gibbs *et al.* and Matsinos *et al.*, and – unlike the original comparisons between these analyses and earlier data – show no evidence for unexpected isospin breaking effects. Further investigations to understand the differences between the CEX cross section predictions would be valuable.

We thank Drs. R. Poutissou and D. Healey for help with the data acquisition and the liquid H<sub>2</sub> target, respectively. We also thank Drs. R. Arndt, W. Gibbs, E. Matsinos and I. Strakovsky for valuable discussions and the National Science Foundation (United States) and the Natural Sciences and Engineering Research Council (Canada) for their financial support.

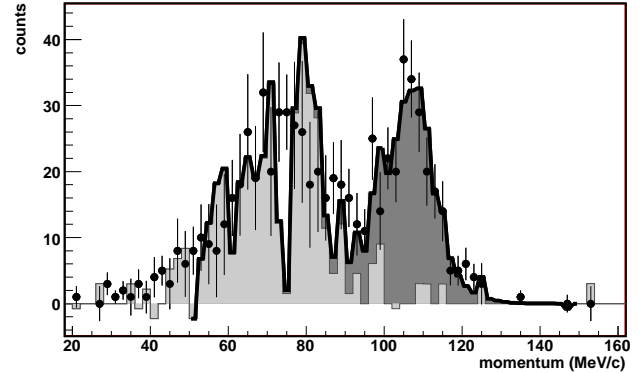


FIG. 1. The  $\pi^0$  momentum spectrum for an incident  $\pi^-$  momentum 104 MeV/c and scattering angles 10-20 deg. The data points (filled circles) are the measured CH<sub>2</sub> spectrum and the solid line is the fit to the sum of the measured ( $\pi^-, \pi^0$ ) background (light gray fill color) and the  $^1\text{H}(\pi^-, \pi^0)$  lineshape (dark gray fill color).

- 
- [1] S. Weinberg, Trans. New York Acad. Sci. **38**, 185 (1977).
  - [2] D.H. Fitzgerald *et al.*, Phys. Rev. C **34**, 619 (1986).
  - [3] L.D. Isenhower *et al.*, PiN Newslett. **15**, 292 (1999).
  - [4] W. R. Gibbs, L. Ai and W. B. Kaufmann, Phys. Rev. Lett. **74**, 3740 (1995).
  - [5] W. R. Gibbs and R. Arceo, Phys. Rev. C **72**, 065205 (2005).
  - [6] E. Matsinos, Phys. Rev. C **56**, 3014 (1997).
  - [7] E. Matsinos, W. S. Woolcock, G. C. Oades, G. Rasche and A. Gashi, Nucl. Phys. A **778**, 95 (2006)
  - [8] A. B. Gridnev, I. Horn, W. J. Briscoe and I. I. Strakovsky, Phys. Atom. Nucl. **69**, 1542 (2006).
  - [9] R. A. Arndt, W. J. Briscoe, I. I. Strakovsky, R. L. Workman and M. M. Pavan, Phys. Rev. C **69**, 035213 (2004).
  - [10] J. Piekarewicz, Phys. Lett. B **358**, 27 (1995).
  - [11] N. Fettes and U. G. Meissner, Nucl. Phys. A **693**, 693 (2001).
  - [12] R. A. Arndt, W. J. Briscoe, I. I. Strakovsky, and R. L. Workman, Phys. Rev. C **74**, 045205 (2006).
  - [13] E. Frléz *et al.*, Phys. Rev. C **57**, 3144 (1998).
  - [14] D.H. Wright *et al.*, Nucl. Instrum. Methods **A320**, 249 (1992).
  - [15] J. Spuller *et al.* Phys. Lett. **67B**, 4 (1977).
  - [16] R. Brun, F. Bruyant, M. Maire, A.C. McPherson and P. Zanarini, GEANT3(1986); CERN report no. DD/EE/84-1 (unpublished).

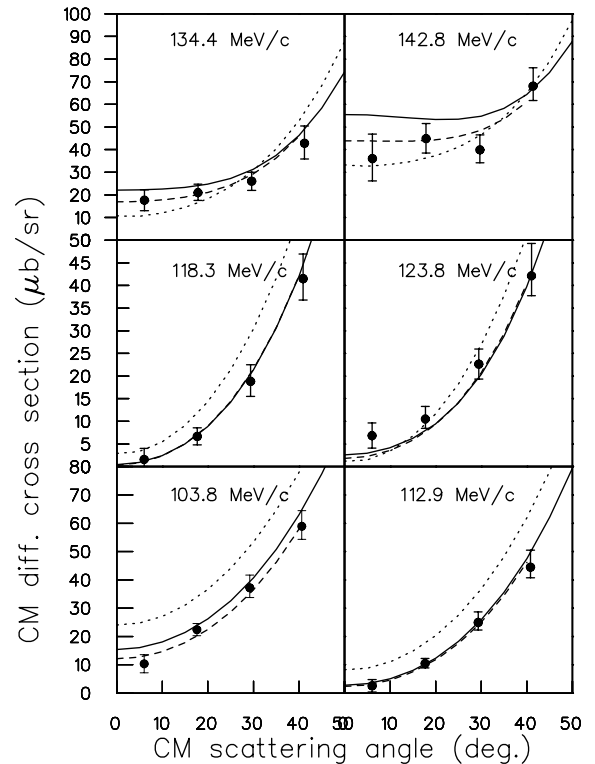


FIG. 2. The  $\pi^- p \rightarrow \pi^0 n$  CM differential cross section versus central momentum and CM angle. The data points are our results. The solid line is the prediction of Gibbs *et al.* [4,5], the dashed line is the prediction of Matsinos *et al.* [7], and the dotted line is the prediction of the GWU group [12].

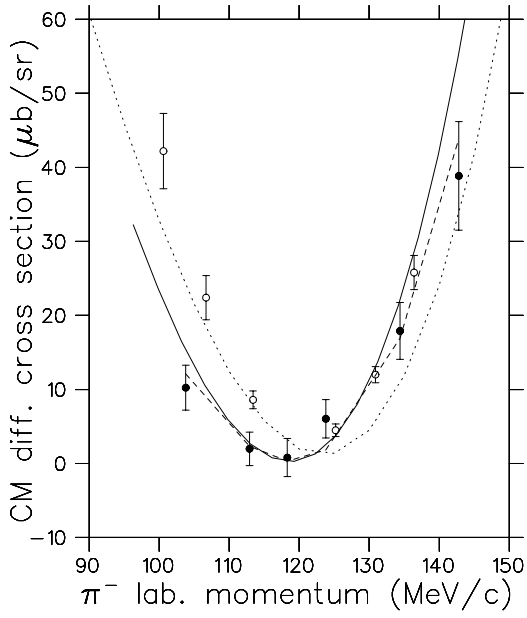


FIG. 3. The zero deg.  $\pi^- p \rightarrow \pi^0 n$  CM differential cross section versus laboratory momentum. The filled circles are our data, the open circles are Fitzgerald's data. The solid line is the prediction of Gibbs *et al.* [4,5], the dashed line is the prediction of Matsinos *et al.* [7], and the dotted line is the prediction of the GWU group [12].